

## New $\beta$ -delayed proton precursors in the rare-earth region near the proton drip line

S.-W. Xu,<sup>1</sup> Z.-K. Li,<sup>1</sup> Y.-X. Xie,<sup>1</sup> Q.-Y. Pan,<sup>1</sup> Y. Yu,<sup>1</sup> J. Adam,<sup>2</sup> C.-F. Wang,<sup>1</sup> J.-P. Xing,<sup>1</sup> Q.-Y. Hu,<sup>1</sup> S.-H. Li,<sup>1</sup> H.-Y. Chen,<sup>1</sup> T.-M. Zhang,<sup>1</sup> G.-M. Jin,<sup>1</sup> Y.-X. Luo,<sup>1</sup> Yu. Penionzhkevich,<sup>2</sup> and Yu. Gangrsky<sup>2</sup>  
<sup>1</sup>*Institute of Modern Physics, Chinese Academy of Sciences, Lanzhou 730000, People's Republic of China*  
<sup>2</sup>*Joint Institute for Nuclear Research, 141980 Dubna, Moscow region, Russia*

(Received 5 April 1999; published 2 November 1999)

The  $\beta$ -delayed proton precursors  $^{125}\text{Nd}$ ,  $^{128}\text{Pm}$ ,  $^{129}\text{Sm}$ ,  $^{137}\text{Gd}$ , and  $^{139}\text{Dy}$  near the proton drip line were produced by the irradiation of  $^{92}\text{Mo}$ ,  $^{96}\text{Ru}$ , and  $^{106}\text{Cd}$  with an  $^{36}\text{Ar}$  beam, and definitely identified for the first time using proton-gamma coincidence in combination with a He-jet tape transport system. Their half-lives were determined to be 0.60(15) s, 1.0(3) s, 0.55(10) s, 2.2(2) s, and 0.6(2) s, respectively. The measured energy spectra of  $\beta$ -delayed protons and estimated proton branching ratios to the final states in “daughter” nuclei were fitted by a statistical model calculation, and then the spins and parities of  $^{125}\text{Nd}$ ,  $^{129}\text{Sm}$ ,  $^{137}\text{Gd}$ , and  $^{139}\text{Dy}$  were preliminarily assigned as  $5/2^\pm$ ,  $1/2^+$  (or  $3/2^+$ ),  $7/2^\pm$ , and  $7/2^+$ , respectively. The agreement between the spin-parity assignments and the predicted Nilsson diagrams indirectly indicates that the ground states of  $^{125}\text{Nd}$ ,  $^{129}\text{Sm}$ ,  $^{137}\text{Gd}$ , and  $^{139}\text{Dy}$  are highly deformed with  $\beta_2 \sim 0.3$ . [S0556-2813(99)50112-X]

PACS number(s): 23.40.Hc, 21.10.Tg, 25.70.Gh, 27.60.+j

Synthesis of new nuclides near the drip line and the study of their exotic decay properties are at the frontier of nuclear physics today. The nuclei along the proton drip line in the rare-earth region speculated by Hofmann [1] or predicted by Möller *et al.* [2] are highly deformed ( $\beta_2 > 0.28$ ) [3]. Therefore, the search for the proton radioactivity from the highly deformed ground state in the rare-earth region has been investigated by many nuclear physicists [4–7] for a long period of time. The search for the proton emission from excited states, i.e., the  $\beta$ -delayed proton ( $\beta p$ ) decay in the region is closely related to the study of the proton radioactivity. It provides fundamental information on both the ground-state properties and the production mechanism for the nuclei near the proton drip line. One of the difficulties encountered in the study of continuous-energy  $\beta p$  from the decay of a precursor near the drip line in the rare-earth region is caused by the isobaric contaminations. In order to identify the precursor unambiguously, additional measurements, such as “ $x$ - $p$ ” coincidence, i.e., the coincidence between the characteristic  $x$  rays of proton emitter and the  $\beta p$ , have to be carried out following a mass separation. However, due to the low electron capture (EC) branching ratio, the “ $x$ - $p$ ” coincidence measurements will reduce the counting rate by one or two orders of magnitude. This fact severely constrains the study of an exotic decay channel with a production cross section as low as 100 nb. In this work we used a different technique to identify the precursors. In the  $\text{EC}/\beta^+$  decay of an even ( $Z$ )-odd ( $N$ )  $\beta p$  precursor, most of the excited-state decays in the even ( $Z-2$ )-even ( $N+1$ ) daughters of each odd ( $Z-1$ )-even ( $N+1$ ) proton “emitter” result in the transition between the lowest-energy  $2^+$  state and  $0^+$  ground state in the “daughter” nucleus. Therefore, the coincidence between  $\beta p$  and the  $2^+ \rightarrow 0^+$   $\gamma$ -ray transition specific for a particular “daughter” nucleus, a “ $p$ - $\gamma$ ” coincidence, can be used to identify the mother, the  $\beta p$  precursor. This method can also be used to identify some of the odd ( $Z$ )-odd ( $N$ ) precursors. In addition, the transportation efficiency of a He-jet tape transport system (HJTTS) for the rare-earth nuclei is higher than the overall efficiency of an isotope separator on line

(ISOL), and the sum of the proton branching ratios ( $b_{\beta p}$ ) to the excited states followed by the  $2^+ \rightarrow 0^+$   $\gamma$ -ray transition in the “daughter” nucleus is larger than the EC branching ratio followed by  $\beta p$  emission. Generally speaking, using the “ $p$ - $\gamma$ ” coincidence in combination with a HJTTS system, the efficiency of measuring the  $\beta p$  specific for a particular precursor in the region can be increased by a factor of 50 in comparison with that using the “ $x$ - $p$ ” coincidence in combination with an ISOL facility. The present paper describes the syntheses and definite identifications of the  $\beta p$  precursors  $^{125}\text{Nd}$ ,  $^{128}\text{Pm}$ ,  $^{129}\text{Sm}$ ,  $^{137}\text{Gd}$ , and  $^{139}\text{Dy}$  for the first time, as well as the preliminary studies of their  $\beta p$  decays by means of the HJTTS+“ $p$ - $\gamma$ ” coincidence.

The experiments were carried out at the National Laboratory of Heavy-Ion Accelerator in Lanzhou (NLHIAL), China. A 220-MeV  $^{36}\text{Ar}^{11+}$  beam from the sector-focused cyclotron of NLHIAL entered a target chamber filled with 1 atm of helium, passing through a 1.94 mg/cm<sup>2</sup> Havar window and a degrader before bombarding different enriched targets:  $^{92}\text{Mo}$  (2.0 mg/cm<sup>2</sup>, 97%),  $^{96}\text{Ru}$  (2.8 mg/cm<sup>2</sup>, 94%), and  $^{106}\text{Cd}$  (2.5 mg/cm<sup>2</sup>, 75%). The beam intensity was about 0.5  $e\mu\text{A}$ . The reaction products stopped in the helium gas were swept through a 6-m-long, 2-mm-diameter plastic capillary to the movable tape in a collection chamber.  $\text{PbCl}_2$  was used as an aerosol with a working temperature of about 430 °C. The radioactivity deposited on the tape was transported periodically to a shielded location for  $p$ - $\gamma_1(x)$ - $\gamma_2(x)$ - $t$  coincidence measurements. Two 570 mm<sup>2</sup> × 350  $\mu\text{m}$  totally depleted silicon surface barrier detectors were used for proton measurements, and located on the opposite two sides of the movable tape. Behind each silicon detector there was a coaxial HpGe (GMX type) detector for  $\gamma(x)$  measurements.

(1)  $^{125}\text{Nd}$ . The measured  $\gamma(x)$ -ray spectrum gated on 2.5–5.5 MeV protons in the  $^{36}\text{Ar}+^{92}\text{Mo}$  reaction is shown in Fig. 1. All of the intense  $\gamma$  lines in Fig. 1 were assigned to their  $\beta p$  precursors except the  $x$  rays and 511-keV  $\gamma$  ray. Among them, the 142- and 306-keV  $\gamma$  lines were assigned to

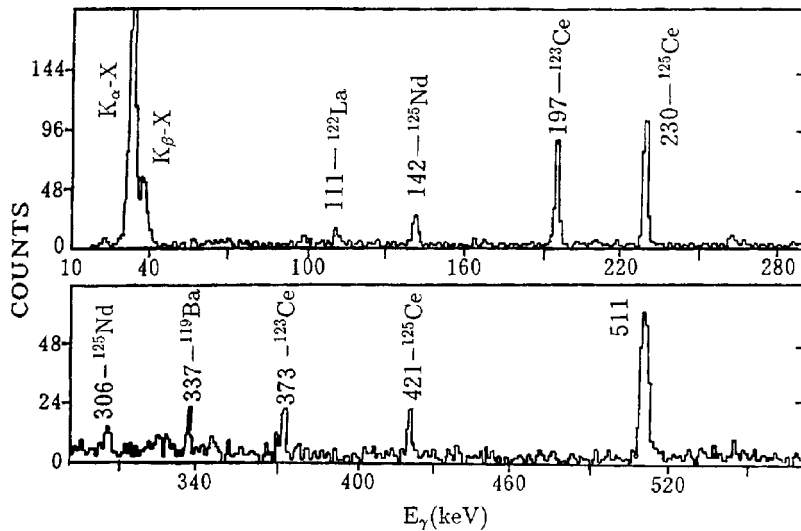


FIG. 1. The measured  $\gamma(x)$  spectrum in coincidence with 2.5–5.5 MeV protons in the  $^{36}\text{Ar} + ^{92}\text{Mo}$  reaction. The intense peaks are labeled with their energies in keV and their  $\beta p$  precursors.

the  $2^+ \rightarrow 0^+$  and  $4^+ \rightarrow 2^+$   $\gamma$  transitions in the “daughter”  $^{124}\text{Ce}$  [8] of the  $\beta p$  precursor  $^{125}\text{Nd}$ . In the  $\gamma(x)$ -ray spectrum gated on both 2.5–6.0 MeV protons and the 142-keV  $\gamma$  ray, only one peak with six events was found with an energy less than 600 keV, and located at 35.8 keV, the energy of the Pr- $K_\alpha$  x ray. It implies that the 142-keV  $\gamma$ -ray transition is related to the decay of an EC/ $\beta^+$ -emitting neodymium isotope. The decay curve of the 142-keV  $\gamma$  line coincident with 2.5–5.5 MeV protons is shown in the inset of Fig. 2(a), from which the half-life of the new nuclide

$^{125}\text{Nd}$  was extracted to be  $0.60 \pm 0.15$  s. In Fig. 1 the intensities of 142- and 306-keV  $\gamma$  lines, as well as the background level at 444 keV, which corresponds to the  $6^+ \rightarrow 4^+$   $\gamma$  transition in  $^{124}\text{Ce}$  [8], were used to estimate the relative  $b_{\beta p}$  to different final states in  $^{124}\text{Ce}$ :  $100(2^+)$ ,  $26 \pm 6(4^+)$ , and  $<3(6^+)$ . The proton energy spectrum gated on the 142-keV  $\gamma$  line is shown in Fig. 2(a), which is the spectrum of the  $\beta p$  from the  $^{125}\text{Nd}$  decay followed by the 142-keV transition in  $^{124}\text{Ce}$ . The component with the energies lower than 2 MeV in the spectrum is attributed to the pileup of positrons in the

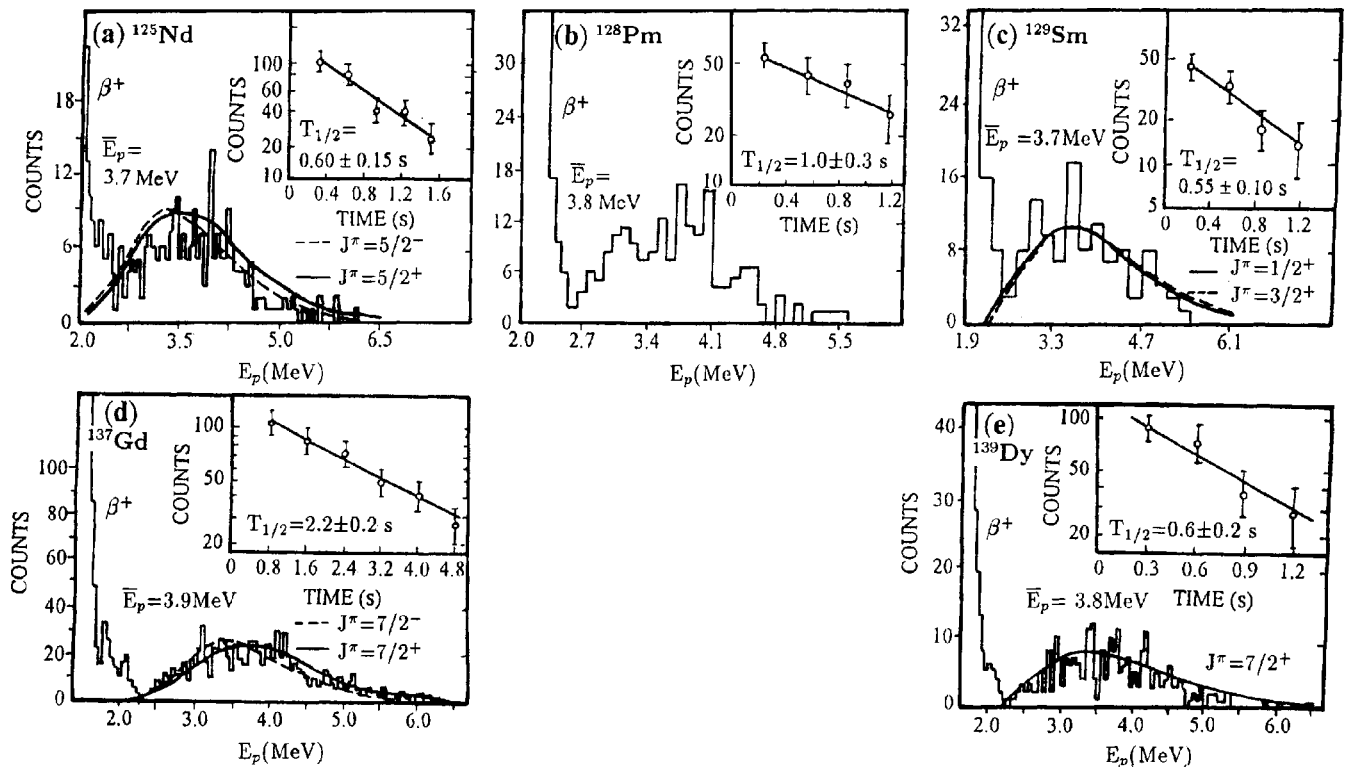


FIG. 2. The observed energy spectra of  $\beta p$  gated by different characteristic gamma rays corresponding to five different precursors. The energies of the characteristic gamma rays for the precursors  $^{125}\text{Nd}$ ,  $^{128}\text{Pm}$ ,  $^{129}\text{Sm}$ ,  $^{137}\text{Gd}$ , and  $^{139}\text{Dy}$  are 142, 326.5, 134, 255, and 221 keV, respectively. The solid and dashed curves were calculated using the statistical model (see text). The insets show the time spectra of the characteristic gamma rays gated on 2.5–5.5 MeV protons.

TABLE I. The production-reaction channels, the partial reaction cross sections via  $\beta p$  decay ( $\sigma_{\beta p}$ ), and the half-lives of  $^{125}\text{Nd}$ ,  $^{128}\text{Pm}$ ,  $^{129}\text{Sm}$ ,  $^{137}\text{Gd}$ , and  $^{139}\text{Dy}$ .

New nuclide	Reaction channel	Bombarding energy (MeV)	$\sigma_{\beta p}^a$ (nb)	Expt. half-life (s)	Theor. Half-life (s)				
					Gross theory [15,16]	Microscopic theory [17]			
					Hilf	Groote	Möller	Möller [2]	
$^{125}\text{Nd}$	$^{36}\text{Ar}+^{92}\text{Mo}$	169	230	$0.60\pm 0.15$	0.67	0.79	0.78	0.58	0.42
$^{128}\text{Pm}$	$^{36}\text{Ar}+^{96}\text{Ru}$	174	50	$1.0\pm 0.3$	0.71	1.8	2.5	1.5	0.40
$^{129}\text{Sm}$	$^{36}\text{Ar}+^{96}\text{Ru}$	165	70	$0.55\pm 0.10$	0.58	0.33	0.62		0.20
$^{137}\text{Gd}$	$^{36}\text{Ar}+^{106}\text{Cd}$	176	450	$2.2\pm 0.2$	1-3				2.0
$^{139}\text{Dy}$	$^{36}\text{Ar}+^{106}\text{Cd}$	176	160	$0.6\pm 0.2$	0.61	0.57	0.65	0.47	0.50

<sup>a</sup>The uncertainty is a factor of 2.

silicon detector. On the other hand, the energy spectrum of  $\beta p$  and the  $b_{\beta p}$  to different final states in  $^{124}\text{Ce}$  were calculated with a revised statistical model [9]. The structureless  $\beta$ -strength function predicted by the gross theory and the energy-level density based on the back-shifted Fermi gas assumption were used in the model calculation. The spins and parities of  $^{125}\text{Nd}$  most consistent with the experimental results are  $5/2^+$ , which give the final state  $b_{\beta p}$  of 67.0 and 65.8 % ( $2^+$ ), 21.4 and 16.3 % ( $4^+$ ), as well as 0.5 and 0.2 % ( $6^+$ ), and reproduce the experimental energy spectrum of  $\beta p$  reasonably well [Fig. 2(a)].

(2)  $^{128}\text{Pm}$ . A 236.5-keV  $\gamma$  line, which corresponds to the  $\gamma$ -ray transition between two low-lying states of  $^{127}\text{Pr}$  [10], appeared in the  $\gamma(x)$ -ray spectrum gated on 2.5–5.5 MeV protons in the  $^{36}\text{Ar}+^{96}\text{Ru}$  reaction. In addition, a clear few-count peak was found at the energy of Nd- $K_\alpha$  x ray in the triple-coincident  $\gamma(x)$ -ray spectrum gated on both 2.5- to 5.5-MeV protons and the 236.5-keV  $\gamma$  line. We assigned the 236.5-keV transition to the “daughter” nucleus  $^{127}\text{Pr}$  produced from the initial ( $\text{EC}/\beta^+$ ) decay of  $^{128}\text{Pm}$  after proton emission. The decay curve of the 236.5-keV  $\gamma$  line in the  $p$ - $\gamma$  coincidence spectrum and the proton energy spectrum gated on the 236.5-keV  $\gamma$  line are shown in Fig. 2(b). From the decay curve the half-life of  $^{128}\text{Pm}$  was extracted to be  $1.0\pm 0.3$  s.

(3)  $^{129}\text{Sm}$ . A 134-keV  $\gamma$  line found in the proton-coincident  $\gamma(x)$ -ray spectrum in the  $^{36}\text{Ar}+^{96}\text{Ru}$  reaction was assigned to the  $\gamma$ -ray transition between the lowest-energy  $2^+$  state and  $0^+$  ground state in the “daughter” nucleus  $^{128}\text{Nd}$  [11] of the  $\beta p$  precursor  $^{129}\text{Sm}$ . The relative  $b_{\beta p}$  to different final states in  $^{128}\text{Nd}$  were estimated to be 100 ( $2^+$ ) and  $<10$  ( $4^+$ ). From the decay curve of the proton-coincident 134-keV  $\gamma$  line [the inset of Fig. 2(c)], the half-life of  $^{129}\text{Sm}$  decay was extracted to be  $0.55\pm 0.10$  s. The spin and parity of  $^{129}\text{Sm}$  most consistent with the experimental results is  $1/2^+$  or  $3/2^+$ , which yield  $b_{\beta p}$  of 54.8% ( $2^+$ ) and 2.5% ( $4^+$ ) or 64.4% ( $2^+$ ) and 4.7% ( $4^+$ ), respectively. These assignments reproduce the experimental energy spectrum of  $\beta p$  equally well [Fig. 2(c)].

(4)  $^{137}\text{Gd}$ . The  $\gamma$  lines with the energies of 255 and 431 keV found in the proton-coincident  $\gamma(x)$ -ray spectrum in the  $^{36}\text{Ar}+^{106}\text{Cd}$  reaction were assigned to the  $2^+\rightarrow 0^+$  and

$4^+\rightarrow 2^+$   $\gamma$  transitions in the “daughter” nucleus  $^{136}\text{Sm}$  [12] of the precursor  $^{137}\text{Gd}$ . From the decay curve of the proton-coincident 255-keV  $\gamma$  line (the inset of Fig. 2(d)), the half-life of the  $^{137}\text{Gd}$  decay was extracted to be  $2.2\pm 0.2$  s. In 1983 the half-life and the energy spectrum of the  $\beta p$  of  $^{137}\text{Gd}$  were measured by Nitschke *et al.* [13] who, however, pointed out that their experimental half-life  $7\pm 3$  s had to be redetermined in a later experiment. The measured half-life of  $^{137}\text{Gd}$  in our experiment is in agreement with the theoretical predictions (see Table I) and with the experimental-value systematics, but is different from Nitschke’s result within the experimental errors. We guess that the energy spectrum of  $\beta p$  observed by Nitschke *et al.* is mixed with a long-life component from another proton emitter. The relative  $b_{\beta p}$  to different final states in  $^{136}\text{Sm}$  were estimated to be 100 ( $2^+$ ),  $51\pm 5$  ( $4^+$ ), and  $<5$  ( $6^+$ ). The spins and parities of  $^{137}\text{Gd}$  most consistent with the experimental results are  $7/2^+$ , which give the final-state  $b_{\beta p}$  of 58.0 and 63.3 % ( $2^+$ ), 26.8 and 28.7 % ( $4^+$ ), as well as 0.8 and 1.2 % ( $6^+$ ), and reproduce the experimental energy spectrum of  $\beta p$  reasonably well [Fig. 2(d)].

(5)  $^{139}\text{Dy}$ . A clear 221-keV  $\gamma$  peak and a tiny 384-keV  $\gamma$  peak in the proton-coincident  $\gamma(x)$ -ray spectrum in the  $^{36}\text{Ar}+^{106}\text{Cd}$  reaction were assigned to the  $2^+\rightarrow 0^+$  and  $4^+\rightarrow 2^+$   $\gamma$  transitions in the “daughter” nucleus  $^{138}\text{Gd}$  [14] of the  $\beta p$  precursor  $^{139}\text{Dy}$ . The relative  $b_{\beta p}$  to different final states in  $^{138}\text{Gd}$  were estimated to be 100 ( $2^+$ ) and  $46\pm 10$  ( $4^+$ ). From the decay curve of the proton-coincident 221-keV  $\gamma$  line [the inset of Fig. 2(e)], the half-life of  $^{139}\text{Dy}$  decay was extracted to be  $0.6\pm 0.2$  s. The spin and parity of  $^{139}\text{Dy}$  most consistent with the experimental results is  $7/2^+$ , which gives final-state  $b_{\beta p}$  of 56.3% ( $2^+$ ) and 30.9% ( $4^+$ ), and reproduces the experimental energy spectrum of  $\beta p$  reasonably well [Fig. 2(e)].

The five new nuclides and their production-reaction channels, partial reaction cross sections of  $\beta p$  and half-lives, including the experimental values and theoretical predictions, are listed in Table I. When we estimated the partial cross sections of  $\beta p$  in column 4 of Table I, the final-state  $b_{\beta p}$  of “daughter” nuclei in  $^{125}\text{Nd}$  ( $5/2^+$ ),  $^{129}\text{Sm}$  ( $1/2^+$ ),  $^{137}\text{Gd}$  ( $7/2^+$ ), and  $^{139}\text{Dy}$  ( $7/2^+$ ) decays were taken from the re-

TABLE II. The observed  $\beta p$  energy regions ( $\bar{E}_p$ ) and centroids of the  $\beta p$  energy spectra, the ground-state quadruple deformations ( $\varepsilon_2$ ), and the spins and parities of  $^{125}\text{Nd}$ ,  $^{128}\text{Pm}$ ,  $^{129}\text{Sm}$ ,  $^{137}\text{Gd}$ , and  $^{139}\text{Dy}$ .

Nucleide	$E_p(\text{MeV})$	$\bar{E}_p(\text{MeV})$	$\varepsilon_2$ [3]	Expt.	Spin and parity			
					Predictions			
					Arseniev [18]	Bengtsson [19]	Audi [20]	Möller [2]
$^{125}\text{Nd}$	2.2-6.2	3.7	0.300	$5/2^+$	$5/2^+$	$5/2^+$		$5/2^+$
$^{128}\text{Pm}$	2.4-5.5	3.8	0.300					
$^{129}\text{Sm}$	2.2-5.5	3.7	0.300	$1/2^+$ , $3/2^+$	$1/2^+$	$1/2^+$		$1/2^+$
$^{137}\text{Gd}$	2.3-6.5	3.9	0.267	$7/2^+$	$7/2^+$	$7/2^+$ , $1/2^-$	$7/2^+$	$9/2^-$
$^{139}\text{Dy}$	2.3-6.0	3.8	0.258	$7/2^+$	$7/2^+$	$7/2^+$	$7/2^+$	$9/2^-$

vised statistical model calculation, and the total  $b_{\beta p}$  followed by the 236.5-keV  $\gamma$  ray in  $^{128}\text{Pm}$  decay was assumed to be 50%. All of the estimated partial cross sections of  $\beta p$  emissions for the five reaction channels listed in Table I are smaller than 500 nb, which indicate the importance of the measurement efficiency. On the whole, the half-lives predicted by Möller *et al.* [2] are slightly shorter than the experimental results.

The information related to the  $\beta p$  and the assignments to the spins and parities of the five precursors, including preliminary experimental results and theoretical predictions is summarized in Table II. The spins and parities in columns 6 and 7 of Table II were taken from the Nilsson diagrams given by Arseniev *et al.* [18] and Bengtsson *et al.* [19], respectively, according to the quadruple deformations ( $\varepsilon_2$ ) in column 4 predicted by the macroscopic-microscopic mass model of Möller *et al.* [3]. The preliminary experimental assignments of spins and parities for  $^{125}\text{Nd}$  and  $^{129}\text{Sm}$  are consistent with all theoretical predictions. The experimental assignments  $7/2^+$  for both  $^{137}\text{Gd}$  and  $^{139}\text{Dy}$  are also consistent with the predicted Nilsson diagrams in Refs. [18,19] and the predictions derived from systematic trends by Audi *et al.* [20]. However, the experimental final-state  $b_{\beta p}$  disagree with the predictions of  $9/2^-$  for both  $^{137}\text{Gd}$

and  $^{139}\text{Dy}$  in Ref. [2]. The theoretical determination of the ground-state spin and parity for an even( $Z$ )-odd( $N$ ) nucleus by means of the orbital occupied by the last neutron in the Nilsson diagram strongly depends on the nuclear deformation. Therefore, the consistency between the experimental spin-parity assignments and the predicted Nilsson diagrams in Refs. [18,19] is an indirect indication that the four nuclides  $^{125}\text{Nd}$ ,  $^{129}\text{Sm}$ ,  $^{137}\text{Gd}$ , and  $^{139}\text{Dy}$  are highly deformed with  $\beta_2 \sim 0.3$ . If  $\beta_2 = 0.3$  and then a lower Coulomb barrier is taken into account, the calculated centroid of the proton energy spectrum ( $\bar{E}_p$ ) by the statistical model shifts to the low-energy side by 0.1–0.2 MeV.

In principle, the proposed identification method can be used to study any  $\beta$ -delayed proton decay. Extending the technique into a different mass region is underway.

We are indebted to Academician of CAS Wei Baowen, Director of NLHIAL for his enthusiastic encouragement and help. This work was supported by the National Natural Science Foundation of China (Grant Nos. 19775056 and 19475055), the Chinese Academy of Sciences and the International Cooperative Program between the National Natural Science Foundation of China and the Russian Foundation of Basic Science.

- [1] S. Hofmann, *Proceedings of the International Conference on the Future of Nuclear Spectroscopy*, Crete, Greece, 1993 (Institute of Nuclear Physics, National Center for Scientific Research Demokritos, 153 10 Aghia Paraskevi, Athens, Greece, 1993), p. 255.
- [2] P. Möller, J.R. Nix, and K.-L. Kratz, *At. Data Nucl. Data Tables* **66**, 131 (1997).
- [3] P. Möller, J.R. Nix, W.D. Myers, and W.J. Swiatecki, *At. Data Nucl. Data Tables* **59**, 185 (1995).
- [4] P.O. Larsson, T. Batish, R. Kirchner, O. Klepper, W. Kurcewicz, E. Roeckl, D. Schardt, W.F. Feix, G. Nyman, and P. Tidemand-Petersson, *Z. Phys. A* **314**, 9 (1983).
- [5] K. Livingston, P.J. Woods, N.J. Davis, A.N. James, R.D. Page, P.J. Sellin, and A.C. Shotton, *Phys. Rev. C* **48**, 3113 (1993).
- [6] *Third IN2P3-RIKEN Symposium on Heavy Ion Collisions*, Shinrin-Koen, Saitama, Japan, 1994, edited by R. Beraud, A. Emsallem, J. Ärje, A. Astier, J. Äystö, D. Rameoud, R. Duffait, J. Genevey, A. Gizon, P. Jauho, Yu. A. Lazarev, Y. Le Coz, N. Redon, and Y. V. Shirokovsky (World Scientific, Singapore, 1995), p. 102; Workshop IGISOL-6, Dubna, Russia, 1997, p. 59.
- [7] C.N. Davids, P.J. Woods, D. Seweryniak, A.A. Sonzogni, J.C. Batchelder, C.R. Bingham, T. Davinson, D.J. Henderson, R.J. Irvine, G.L. Poli, J. Unsitalo, and W.B. Walters, *Phys. Rev. Lett.* **80**, 1849 (1998).
- [8] H. Iimura, J. Katakura, K. Kitao, and T. Tamura, *Nucl. Data Sheets* **80**, 895 (1997).
- [9] P. Hornshøj, K. Wilsky, P.G. Hansen, B. Johson, and O.B. Nielsen, *Nucl. Phys. A* **187**, 609 (1972); J.C. Hardy, *Phys. Lett.* **109B**, 242 (1982).
- [10] A.N. James, T.P. Morrison, P.J. Nolan, D. Watson, K.L. Ying, T.P. Connell, and J. Simpson, *Nuclear Structure Appendix*,

- Daresbury Annual Report 1985/86, p. 103.
- [11] R. Moscrop, M. Campbell, W. Gelletly, L. Goettig, C.J. Lister, and B.J. Varley, Nucl. Phys. **A499**, 565 (1989).
- [12] E.S. Paul, S. Davis, P. Vaska, P.J. Bishop, S.A. Forbes, D.B. Fossan, Y.-J. He, J.R. Hughes, I. Jenkins, Y. Liang, R. Ma, M.S. Metcalfe, S.M. Mullins, P.J. Nolan, R.J. Poynter, P.H. Regan, R. Wadsworth, and N. Xu, J. Physiol. (London) **G19**, 861 (1993).
- [13] J.M. Nitschke, M.D. Cable, and W.D. Zeite, Z. Phys. A **312**, 265 (1983).
- [14] C.J. Lister, B.J. Varley, R. Moscrop, W. Gelletly, P.J. Nolan, D.G. Love, P.J. Bishop, A. Kirwan, D.J. Thornley, L. Ying, R. Wadsworth, J.M. O'Donnell, H.G. Price, and A.H. Nelson, Phys. Rev. Lett. **55**, 810 (1985).
- [15] K. Takahashi, M. Yamada, and T. Kondoh, At. Data Nucl. Data Tables **12**, 101 (1973).
- [16] T. Horiguchi, T. Tachibana, and J. Katakura, Chart of the Nuclides, 1996.
- [17] M. Hirsch, A. Staudt, K. Muto, and H.V. Klapdor-Kleingrothaus, At. Data Nucl. Data Tables **53**, 165 (1993).
- [18] D.A. Arseniev, A. Sobiczewski, and V.G. Soloviev, Nucl. Phys. **A126**, 15 (1969).
- [19] T. Bengtsson and I. Ragnarsson, Nucl. Phys. **A436**, 14 (1985); R.B. Firestone, in *Table of Isotopes*, 8th ed., edited by V.S. Shirley, C.M. Baglin, S. Y. Frank Chu, and J. Zipkin (Wiley, New York, 1996), Vol. II, Appendices H, H3.
- [20] G. Audi, O. Bersillon, J. Blachot, and A.H. Wapstra, Nucl. Phys. **A624**, 1 (1997).